

Short Communication

Mechanisms of Microwave Absorption in Carbon Compounds from Shungite

S. Emelyanov<sup>1</sup>, A. Kuzmenko<sup>1</sup>, V. Rodionov<sup>1</sup>, M. Dobromyslov<sup>2</sup>

<sup>1</sup> Southwest State University, 94, 50 Let Oktyabrya Str., 305040 Kursk, Russia

<sup>2</sup> Pacific National University, 136, Tihookeanskaya Str., 680035 Khabarovsk, Russia

(Received 24 October 2013; published online 10 December 2013)

According to SEM, X-ray phase analysis, Raman scattering data features of nanostructural changes in shungite carbon structure were found when processing shungite in 52 % hydrofluoric acid. It is found that conductivity increases up to the values of electrical graphite and absorption of microwave radiation also increases at frequencies up to 40 GHz, which, along with dielectric losses, is due to intense processes of both scattering at laminar carbon structures and absorption of electromagnetic energy.

**Keywords:** Scanning electron microscopy, X-ray diffraction, Small-angle X-ray scattering, Raman scattering spectroscopy, Mapping of Raman shift distributions, Microwave absorption, Shungite.

PACS numbers: 07.78. + s, 07.85.Fv, 42.65.Dr, 07.57. – c

1. INTRODUCTION

Micro- and nanostructural features of naturally-doped minerals-shungites that have particles not greater than 100 nm in size and coherent scattering areas of several nanometers are of interest for studying the attenuation mechanisms in microwave range [1, 2]. So mechanically and chemically disintegrated shungites from Sazhugin deposits have been studied according to the procedure described in [3] with the chemical processing  $6HF + SiO_2 \rightarrow H_2[SiF_6] + 2H_2O$ .

2. EXPERIMENTAL SECTION

Element distribution in cleavages of chosen samples (JEOL JSM6610LV, EDX Oxford Instruments) was typical and is given in Fig. 1a-d with mapping data with a resolution of 1  $\mu m$ . After chemical processing the structure turned delaminated, and the particles became oval with an average diameter of up to 100  $\mu m$  (Fig 2a). The carbon content, according to increase by 6 %. The increase in content of metals occurs and the silicon content dropped off ten-fold.

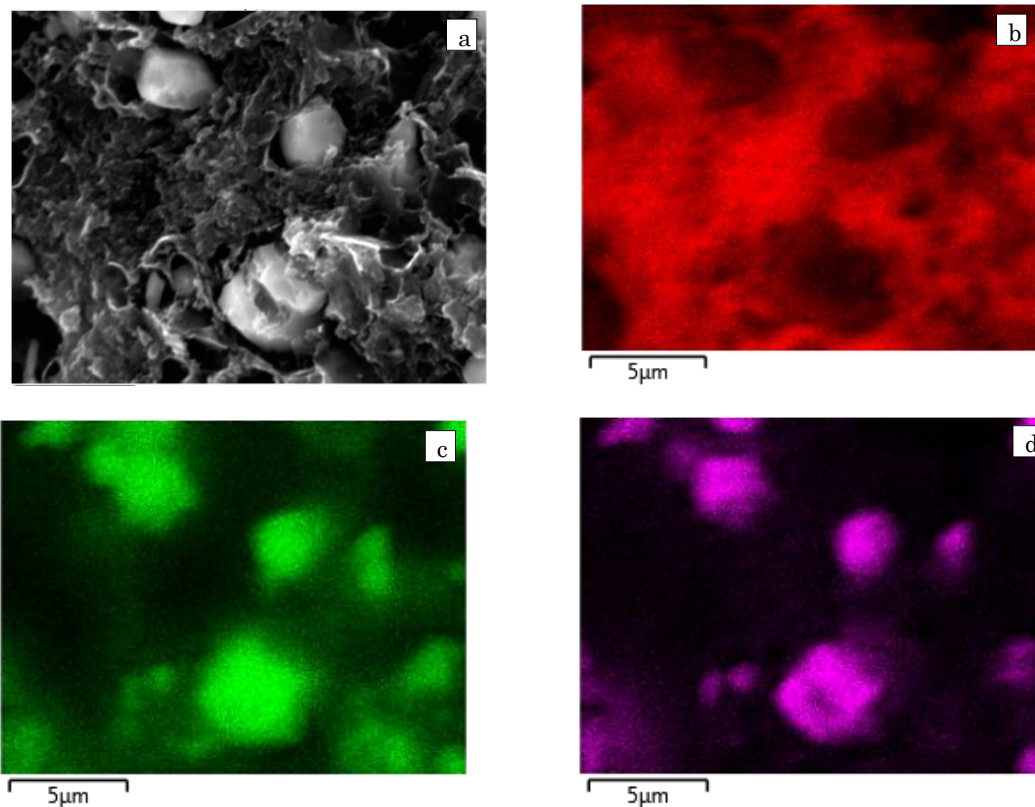
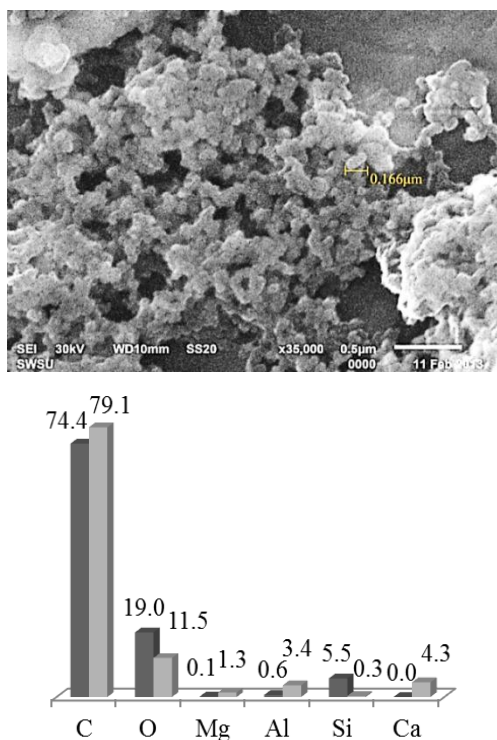
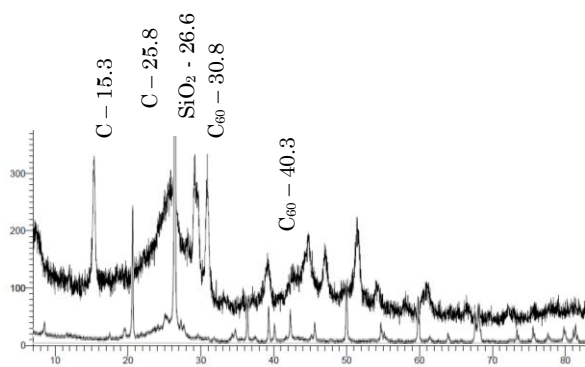


Fig. 1 – SEM-images of shungite (a) with a resolution of 1  $\mu m$  with elemental contrast: b – C, c- Si, d- O



**Fig. 2** – SEM of HF processed shungite powder (top). Elemental composition (%) before (black) and after processing (grey) (bottom)



**Fig. 3** – X-ray patterns of shungite before and after processing

Analysis of shungite phase composition (GBC EMMA,  $\text{CuK}_\alpha$ ) before and after processing is given in Fig. 3. It is found that it belongs to shungites of the 1 type (reflection in the neighborhood of  $2\theta \sim 80^\circ$  [2]). The reflections of all modifications of quartz and carbon structures typical of shungite were observed. Using diffraction patterns before and after processing the sizes of carbon nanostructures have been calculated (the coherent scattering areas ( $L$ ) of X-ray radiation) from the Scherer equation:  $L = k\lambda / (B \cos \theta)$ . The reflection width was considered by the level 0.5 ( $B$ ),  $\theta$  is the Bragg angle,  $\lambda = 0.154178$  nm for  $\text{CuK}_\alpha$ ,  $k$  is a constant equal to 0.9 for reflections to the plane (002) and 1.84 to the plane (10) according to [2]. For the plane (100) we adopted  $k = 1.4$ . The predicted sizes of  $L$  are shown in Table 1 in comparison both with sizes in [2] and those according to small-angle X-ray scattering data (SAXSees  $\text{mc}^2$ ,  $\text{CuK}_\alpha$ ).

**Table 1** – Predicted sizes of carbon nanostructures

| Samples          | $B$ , degree | $2\theta$ , degree | $L_{100}$ , nm |
|------------------|--------------|--------------------|----------------|
| Initial          | 4.5          | 26                 | 3.6            |
| After HF         | 8.0          | 26                 | 5.5            |
| According to [2] | 3.9          | –                  | 5.4            |
| SAXSees          | –            | –                  | 5.1            |

Raman scattering spectra on samples before and after processing shungite were examined with a resolution of 500 nm with a spectral resolution of up to  $0.8 \text{ cm}^{-1}$  (OmegaScope, SmartSPM) and are shown in Fig. 4. In this case excited were lines  $D - A_{1g}$  ( $1354 \text{ cm}^{-1}$ ) – vibration of the whole carbon structure and  $G - E_{2g}$  ( $1593 \text{ cm}^{-1}$ ) – antisymmetric vibration of carbon structures and the second order lines  $2D - 2688$  and  $2G - 2916 \text{ cm}^{-1}$ . The amorphization level  $K$  by the variation of  $I_D - A_{1g}$  и  $I_G - E_{2g}$ :  $K = (I_D + I_G) / (I_D - I_G)$  in shungite before and after processing was  $\sim 5$  и  $\sim 8$ , respectively. The lines of fullerenes  $450$  and  $190 \text{ cm}^{-1}$  with their content of up to 2 % were found in Raman spectra by mapping the cleavage surfaces of shungite (scans of 900 spectra  $60 \times 60 \mu\text{m}$ ).

Conductivity of shungite samples in the form of pressed tablets ( $220 \text{ atm}$ ,  $1 \div 10 \times 20 \text{ mm}$ ) examined with the LCR-meter Instek LCR-819 is characterized by an order of magnitude increase, up to the value for ordinary graphite. Nonlinear increase is observed to 600 K and a succeeding saturation in the range measured to 800 K. All samples are characterized by high absorbing capacity (Fig. 5a, b) of microwave radiation (PNA-L Agilent N5230A,  $12.6 - 40 \text{ GHz}$ ).

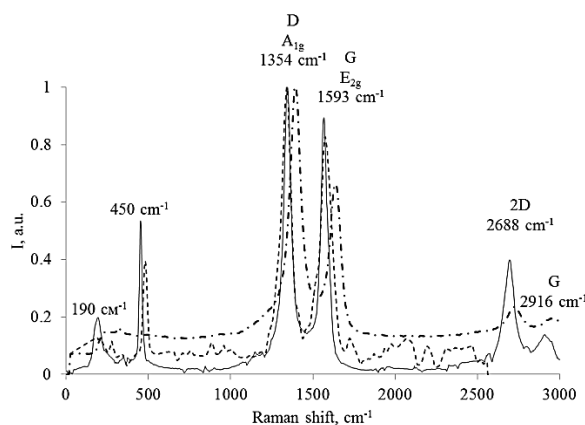


**Fig. 4** – Raman spectra of shungite before (— · — · —) and after HF processing (— — —). One of 900 scans of Raman scattering with lines  $C_{60}$  (—)

### 3. RESULTS AND DISCUSSION

The transmission coefficient within the range 19.6 and 21.7 GHz was equal on average to  $-21$  dB, and on 29.1 GHz – 39 dB. The shungite transmission coefficient  $S_{21}$  is probably due to multiple reflections and absorptions within laminar carbon structures (Fig. 2). This fact is also indicated by the observed decrease in  $S_{21}$  for the sample from  $-9.5$  dB to  $-44.5$  dB at 13.6 GHz and 38.5 GHz, respectively,

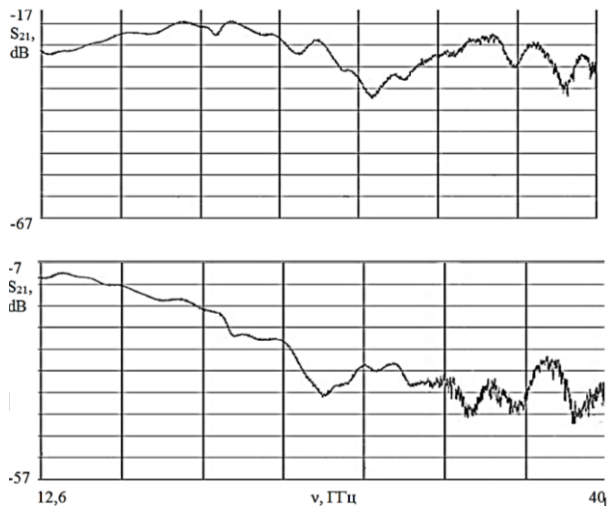


**Fig. 5** – Amplitude-frequency characteristic of  $S_{21}$  before (top) and after HF processing (bottom) of shungite

that is more than 4.5-fold. The depth of skin layer for microwave radiation:  $\delta = (\pi f \xi \sigma)^{-1/2}$  ( $f$  is frequency of electromagnetic radiation,  $\xi = \mu_0 \mu^*$  is suppressor penetrability,  $\mu_0$  is permeability of vacuum,  $\sigma$  is electroconductivity) turns out to be much greater than the sizes of nanocarbon laminar structures, which adds to multiple reflections. Also, as shown in Fig. 5, the surface eddy currents grow. When  $R_C \gg R_{Me}$ , the Joule heat loss increases.

#### 4. CONCLUSIONS

Thus, the increase of microwave radiation absorption in derivatives from shungite carbon structures, in addition to dielectric losses, is due to intense processes of both scattering and absorption of electromagnetic energy.

#### REFERENCES

1. F. Qin, C. Brosseau, *J. App. Phys.* **111**, 061301 (2012).
2. V.V. Kovalevski, P.R. Buseck, J.M. Cowley, *Carbon* **39**, 243 (2001).
3. A.P. Kuzmenko, V.M. Emelianov, V.E. Dreizin, S.A. Efanov, V.V. Rodionov, *Proceedings of the Southwest State University* **2** (2012).